0090-9556/97/2508-0903–911$02.00/0
DRUG METABOLISM AND DISPOSITION
Vol. 25, No. 8
Printed in U.S.A.

SCALING FACTORS TO RELATE DRUG METABOLIC CLEARANCE IN HEPATIC MICROSOMES, ISOLATED HEPATOCYTES, AND THE INTACT LIVER

Studies with Induced Livers Involving Diazepam

DAVID J. CARLILE, KATAYOUN ZOMORODI,[1] AND J. BRIAN HOUSTON

School of Pharmacy and Pharmaceutical Sciences, University of Manchester

(Received May 22, 1996; accepted April 30, 1997)

ABSTRACT:

Microsomal protein recovery and hepatocellularity have been determined and investigated as scaling factors for interrelating clearance by hepatic microsomes, freshly isolated hepatocytes and whole liver from untreated (UT) rats and rats treated with either the cytochrome P450 inducer phenobarbital (PB) or dexamethasone (DEX). Hepatocellularity in UT rats (1.1×10^8 hepatocytes/g liver) was not significantly different after either PB or DEX induction (1.1 and 1.3×10^8 hepatocytes/g liver, respectively). However the microsomal protein recovery index, which provides a scaling factor that is inversely related to the efficiency of the microsomal preparation procedure, was 47 mg/g liver in both PB and DEX microsomes and differs from UT rats (60 mg/g liver). These contrasting findings are consistent with the interlaboratory trends in the literature, indicating that, although hepatocellularity estimates are in good accord, microsomal recovery can vary 2-fold; this has implications for scaling.

The oxidation of diazepam to its three primary metabolites was measured in PB and DEX microsomes and hepatocytes and the scaling factors were applied to these data and previously reported UT data. Marked changes in kinetics occur on induction resulting in a shift in the major pathway. In particular, 3-hydroxylation is induced over 20-fold by DEX. Diazepam CL_{int} was determined *in vivo* after administration of a bolus dose into the hepatic portal vein of UT, PB, and DEX rats; values of 127, 191, and 323 ml/min/SRW (where SRW is a standard rat weight of 250 g), respectively, were obtained. Using these scaling factors, the hepatocyte predictions of CL_{int} were excellent (99, 144, and 297 ml/min/SRW for UT, PB, and DEX, respectively), whereas only the DEX prediction (248 ml/min/SRW) was accurate for the microsomal system, with a substantial underprediction for UT and PB (46 and 68 ml/min/SRW, respectively). Evidence is presented for product inhibition, resulting from accumulation of primary metabolites within the microsomal preparation, as the mechanism responsible for this underprediction.

These results illustrate that the scaling factor approach is applicable to induced livers in which both cytochrome P450 complement and zonal distribution are altered. These data, together with our previous studies, demonstrate that CL_{int} in cells (2.4–297 ml/min/SRW), microsomes (2.7–248 ml/min/SRW), and *in vivo* (1.5–323 ml/min/SRW) are related in a linear fashion and hence inherently both *in vitro* systems are of equal value in predicting *in vivo* CL_{int}.

The use of scaling factors in drug metabolism provides an approach to compare directly kinetic data from two or more *in vitro* systems and to predict *in vivo* behavior from *in vitro* systems. These factors should not be purely empirical in nature, rather they should originate from the anatomical and/or biochemical characteristics of the *in vitro* system. For example, hepatic microsomal rates of metabolism are usually expressed per milligram of microsomal protein and may be scaled by recognizing the inefficiency of the microsomal isolation procedure by using a microsomal recovery factor. This recovery factor enables the conversion of rates to units of liver weight and hence to the intact animal. Similarly, hepatocyte suspension data, expressed per million cells, require a hepatocellularity number to render such data comparable with other *in vitro* systems or predictive of the *in vivo* situation.

In assessing the utility of scaling factors using a data base of 25 drugs (1), we found excellent *in vivo* prediction of metabolic clearance from both microsomes and hepatocytes for low clearance drugs. However, whereas the prediction for high clearance drugs from hepatocytes proved to be equally valuable, underestimation of *in vivo* high clearance from microsomal data was frequently observed. Further comparison of the relationship between microsomal and hepatocellular clearance suggested that a maximum limit for microsomal clearance may exist. However, because the data used in this later analysis originated from a variety of laboratories, no definitive conclusions could be drawn. In contrast, the main analysis clearly demonstrated the value of microsomal protein recovery index and hepatocellularity as microsomal and hepatocyte scaling factors, respectively.

To examine further the scaling factor approach, we have now investigated the scaling of data from hepatic microsomes and hepatocytes from PB[2]- and DEX-treated Sprague-Dawley rats, together

This study was supported by the Biotechnology and Biological Sciences Research Council and the Wellcome Research Laboratories. A portion of this study was presented at the meeting of the British Pharmacological Society, April 5–7, 1995, Canterbury, UK, and appeared in abstract form in *Br. J. Clin. Pharmacol.* **40,** 181P (1995).

[1] Present address: Department of Anesthesia, Stanford University, Stanford, CA.

Send reprint requests to: Dr. J. Brian Houston, School of Pharmacy and Pharmaceutical Sciences, University of Manchester, Oxford Road, Manchester M13 9PL, UK.

[2] Abbreviations used are: PB, phenobarbital; DEX, dexamethasone; UT, untreated; CYP, cytochrome P450; DZ, diazepam; 4′-HDZ, 4′-hydroxydiazepam; 3-HDZ, 3-hydroxydiazepam; NDZ, nordiazepam; SRW, standard rat weight; 3-HNDZ, 3-hydroxynordiazepam; CL_{int}, intrinsic clearance; MRT, mean residence

with analogous data from UT animals. Treatment with CYP inducers such as PB and DEX produces a number of effects in the liver, including the induction of members of the CYP2B and CYP3A subfamilies (2, 3). In addition to altering the CYP complement, both PB and the DEX-type inducer pregnenolone-16α-carbonitrile (4) are known to change the zonal CYP distribution (5). To assess the consequences of induction, DZ was used as the substrate because the formation of its three primary metabolites—4′-HDZ, 3-HDZ, and NDZ—is substantially, yet selectively, affected by PB and DEX treatment (6). Several studies have indicated that 3-HDZ formation is mediated by the CYP3A subfamily (6–8), which is inducible by DEX (3) and to a lesser extent by PB (2). There are conflicting reports (6–8) regarding which CYP isoforms are responsible for NDZ formation; however, CYP2B, CYP2C, and CYP3A have been implicated. Also, Neville and coworkers (7) have demonstrated that 4′-HDZ formation is principally mediated by CYP2D1, an isoform believed to be noninducible by either PB or DEX.

The aims of the present studies are therefore 2-fold: *1*) to extend the scaling factor approach to livers of varying CYP complement and zonal distribution; and *2*) to assess whether there is a progressive increase in both microsomal and hepatocellular clearance of DZ in the induced state, which is predictive of the *in vivo* situation. In the UT rat the clearance of DZ is high: 174 ml/min/SRW (9). Thus, the use of induced systems extends substantially the range of clearances previously investigated in the authors' laboratory for *in vitro:in vivo* comparisons.

Materials and Methods

Chemicals. 3-HDZ and prazepam were generously supplied by Wyeth (Maidenhead, Berks, UK), 4′-HDZ, and 3-HNDZ were gifts from Roche Ltd. (Welwyn Garden City, Herts, UK) and the Warner Co. (Pontypool, Gwent, UK), respectively. NDZ and DZ were purchased from Sigma (Poole, Dorset, UK). All other chemicals were obtained from either BDH (Lutterworth, Leicester, UK) or Sigma.

Animals and Treatment. Male Sprague-Dawley rats (220–250 g) were obtained from the Biological Sciences Unit at the University of Manchester. They were housed 2–4 per cage on sawdust bedding in rooms maintained at a temperature of 20 ± 2°C and allowed free access to water and Chow Rat Mouse rat diet. Rats were either UT or administered intraperitoneal injections of PB (80 mg/kg in 0.9% saline) or DEX (100 mg/kg in 2% Tween 80) once daily for 3 days, with death on the fourth day. In each case, the animals were divided into three groups for either microsomal ($N = 4$ for each inducer), hepatocyte ($N = 4$ for each inducer), or *in vivo* ($N = 5$ for PB/DEX). To complement the latter case, an additional group of control rats received corresponding injections of 2% Tween 80 ($N = 3$).

Microsomal Studies. PB- and DEX-treated rats were killed by cervical dislocation, and the livers were excised and washed in ice-cold potassium chloride (0.15 M). Livers were subsequently homogenized in ice-cold buffer (0.25 M sucrose, 1 mM EDTA, and 25 mM Trizma base; pH 7.4) to yield a liver homogenate tissue concentration of 0.33 g/ml. Washed microsomes were prepared as described previously (10). Liver homogenate and microsomal CYP and protein contents were determined using the methods of Omura and Sato (11) and Lowry *et al.* (12), respectively. Liver homogenate DNA content was determined using the method of Downs and Wilfinger (13).

For the determination of Michaelis-Menten parameters, microsomal incubation conditions with DZ were as detailed previously (9), ensuring linearity between rates of formation and time and microsomal protein concentration. The effects of the primary metabolites as product inhibitors of DZ metabolism were investigated by the same methodology at a DZ concentration of 2 μM and an exogenous metabolite concentration (either 4′-HDZ, 3-HDZ, or NDZ) of 100 μM. Total DZ metabolism was assessed by substrate depletion after an incubation time of 15 min.

Hepatocyte Studies. Hepatocytes were prepared as described elsewhere (10) from PB- and DEX-treated rats. Cell protein and CYP content were estimated as described for microsomes. The DNA content of cells was determined after freshly isolated hepatocytes had been disrupted by the addition of a detergent buffer as detailed by Dunn and coworkers (14). Cell protein content was determined after the digestion of cells in 0.5 M sodium hydroxide; cell CYP content was estimated in cells disrupted by homogenization. Cell numbers in all drug incubations refer to hepatocytes only. The incubation conditions to achieve metabolism and hydrolyze conjugates before analysis were as described previously (9), ensuring linearity of rates of metabolism with respect to time and cell density.

Analysis of DZ Metabolites. The method of Reilly *et al.* (6) was used to assay 4′-HDZ, 3-HDZ, and NDZ in the microsomal and hepatocyte incubates as described previously (9).

***In Vivo* Studies.** Polyethylene cannulae were inserted into the lineal vein (15) and right carotid artery (16) under halothane anesthesia in DEX-treated ($N = 5$), PB-treated ($N = 5$), and control ($N = 3$) rats after the third daily injection of either DEX, PB, or vehicle alone. Animals were subsequently housed one per cage and allowed 1 day to recover from this procedure. DZ [10 mg/kg in propane-1,2-diol, ethanol, and 0.9% saline (40%:10%:50%, v/v/v)] was administered (2 ml/kg) into the hepatic portal vein *via* the lineal vein as a 5-min infusion. Blood samples ($N = 9$) were taken from the carotid artery over a 90-min period, and plasma separated by centrifugation and analyzed for DZ as detailed elsewhere (9).

Data Analysis. The Michaelis-Menten equation was used to determine the V_{max} and K_M values for each pathway of DZ metabolism using the Siphar nonlinear regression software (Simed, Cretéil, France). Goodness of fit was judged by visual inspection of the line of best fit, consideration of the randomness of the residuals, the standard error of the parameter estimates (<20%), and the Aikaike information criteria. Because the substrate loss in both the microsomal and hepatocyte incubations calculated from the initial rate of metabolite formation was substantial, the logarithmic mean of the initial and final substrate concentrations was used as the independent variable in the curve-fitting procedure.

Hepatocellularity was calculated by three methods based on the ratios of liver/cell protein, DNA, or CYP. The liver comprises ~65% hepatocytes, which occupy 80% of the cellular volume (5). However, the hepatocyte isolation procedure, involving filtration and low-speed centrifugation, yields a cell suspension of which hepatocytes comprise ~90% (17, 18). Steinberg *et al.* (18) demonstrated that hepatocytes contain 97% of the total protein in liver tissue and, that in an isolated cell suspension, 99% of the protein is contained in hepatocytes. Therefore, strictly speaking, the ratio of liver to cell protein should be corrected by these factors (0.97/0.99; *i.e.* 0.98); however, this was considered unnecessary. Similarly, the calculation of hepatocellularity by CYP content was also based directly on the liver/cell CYP ratio. The use of DNA to calculate hepatocellularity requires consideration not only of the percentage of hepatocytes in both the isolated cell suspension and the whole liver, but also the binuclearity of ~20% of hepatocytes (17). The percentage of hepatocellular DNA in the whole liver is 69%, whereas the corresponding value in the isolated cell suspension is 92%, therefore the liver/cell DNA ratio was corrected by 0.75 (0.69/0.92).

Microsomal protein recovery ratio (mg protein/g liver) was estimated from the ratio of liver homogenate CYP content (nmol/g liver) to microsomal CYP content (nmol/mg protein). No correction for nuclear or other nonmicrosomal CYP was made because it has been demonstrated that microsomal CYP accounts for >95% of hepatocyte CYP content, even following PB treatment (19, 20).

CL_{int} was calculated from the V_{max}/K_M ratio and scaled to *in vivo* by multiplying by either the microsomal protein recovery ratio or hepatocellularity as the scaling factor. Scaling factors are reported in the text and refer to a SRW of 250 g, with a liver weight of 11 g. Extension of the use of scaling factors to induced livers involves some particular considerations due to the morphological changes known to occur. It is well documented that PB administration to rats causes an increase in liver weight as a result of smooth endoplasmic reticulum proliferation (21). There is also an increase in nuclear DNA, although this is due to increases in ploidy rather than hepatocyte number

time; *CL*, clearance; V_{SS}, volume of distribution at steady-state; CL_{IP}, intraportal clearance; B/P, blood:plasma ratio; *fu*, fraction of unbound drug concentration.

(21). Therefore, for scaling purposes in the induced state, it seems reasonable to assume that the total number of cells per liver remains unaltered and thus an SRW of 250 g should apply.

In vivo estimates of CL_{int} were obtained from the clearance term after administration *via* the intraportal route. A biexponential zero-order input model was used to fit the *in vivo* plasma concentration data (eq. 1) and the pharmacokinetic parameters MRT, CL, and V_{SS} were calculated from eqs. 2–4, respectively:

$$C = R_0 \sum_{i=1}^{n} \left(\left[\frac{1 - e^{+\theta\lambda_i}}{-\lambda_i} \right] C'_i e^{-\lambda_i t} \right), \quad (1)$$

where C is the concentration, λ_i is the rate constant, $C'_i = C_i/\text{DOSE}$, t is the time, and $\theta = t$ for $t \leq \tau$ or $\theta = \tau$ for $t > \tau$ (R_0 and τ are infusion rate and duration, respectively).

$$\text{MRT} = \frac{\text{AUMC}}{\text{AUC}}, \quad (2)$$

where AUMC and AUC are areas under moment curve and concentration curve, respectively.

$$CL = \frac{\text{DOSE}}{\text{AUC}} \quad (3)$$

$$V_{SS} = \text{CL} \cdot \text{MRT} \quad (4)$$

Plasma sampling was conducted for >75 and 90 min for DEX and PB/control rats, respectively, which corresponded to approximately three terminal half-lives and limited the extrapolated AUC to 12%.

CL_{int} was calculated from CL, B/P, and fu, as shown in eq. 5.

$$CL_{int} = \frac{CL}{fu \cdot \text{B/P}}. \quad (5)$$

Results were statistically analyzed using either one-way ANOVA or the Student's t test as appropriate. Results are presented as means ± SD.

Results

***In Vitro* Hepatocyte Studies.** The production of all three primary DZ metabolites demonstrated monophasic Michaelis-Menten kinetics in PB and DEX hepatocytes as shown in fig. 1. In both induced states, the 3-HDZ pathway dominates in contrast to UT (table 1). Substantial formation of NDZ and 4′-HDZ also occurred; however, the secondary metabolite 3-HNDZ was not observed during the 10-min incubation.

PB treatment caused a significant increase in the V_{max} values for both the 3-HDZ and NDZ pathways, whereas the corresponding value for the 4′-HDZ pathway was unchanged, compared with UT. There was a concomitant increase in CL_{int} for the former two pathways, whereas the CL_{int} for the 4′-HDZ pathway was reduced as a result of an increase in the K_M (table 1). The CL_{int} of the 3-HDZ pathway increased ~9-fold in DEX hepatocytes as a consequence of a 3-fold change in both V_{max} and K_M. The NDZ pathway CL_{int} also increased after treatment with this inducer in a comparable manner to PB treatment, whereas 4′-HDZ formation was unaffected by DEX treatment. Figure 2 illustrates the qualitative changes in the relative importance of the three pathways that occur on PB and DEX induction. There is a large increase in the contribution of the 3-HDZ pathway to CL_{int}, whereas the 4′-HDZ pathway contribution is reduced and the NDZ pathway is relatively unaffected.

***In Vitro* Microsomal Studies.** Rates of primary metabolite formation in both PB and DEX microsomes also demonstrated single-site Michaelis-Menten kinetics (fig. 1). Again, only the three primary metabolites were formed in the time course of the study (5 min).

The net effect of these inducers, as shown in table 1, was an increase in the importance of both the 3-HDZ and NDZ routes of DZ metabolism, the largest change occurring for the former pathway. Neither CYP inducer had any effect on the 4′-HDZ pathway. PB microsomes exhibited a 3-fold increase in both the 3-HDZ and NDZ V_{max} values, thereby significantly increasing the CL_{int} of these pathways, compared with the UT data. DEX treatment also resulted in increases in the V_{max} for 3-HDZ and NDZ in addition to significant decreases in the K_M values of both of these pathways, with the major change being a 21-fold increase in the 3-HDZ CL_{int}.

Qualitatively, the effects of induction were similar with respect to each pathway in both *in vitro* systems (fig. 2). There were no significant differences in K_M values between microsomes and hepatocytes for the 4′-HDZ and NDZ pathways, whereas the 3-HDZ pathway K_M was significantly lower in hepatocytes of each treatment state. The rank order of K_M values was consistently 4′-HDZ < NDZ < 3-HDZ (table 1).

Determination of Hepatocyte and Microsomal Scaling Factors. To obtain appropriate hepatocyte scaling factors, hepatocellularities based on both the DNA and protein contents of liver homogenate and isolated hepatocytes were determined in UT, PB, and DEX rats (table 2). Neither inducer had any significant effect on either the protein or DNA content of liver and isolated cells, although the hepatocellularities determined using the protein methodology were significantly higher than the corresponding DNA determined values. In contrast, the microsomal scaling factor, based on microsomal protein recovery, was altered after PB and DEX treatments (table 3) and was significantly reduced in both populations of induced microsomes compared with UT.

Comparison of Predicted CL_{int} from Hepatocyte and Microsomal Studies. The *in vitro* PB and DEX data obtained in the present study and the UT data reported previously (9) were scaled using the above scaling factors to obtain estimates of CL_{int} (as shown in table 4). These results confirm that 3-HDZ formation is the major determinant of DZ disposition in both *in vitro* systems after either PB or DEX treatment, whereas 4′-HDZ production is the major route of DZ CL_{int} in UT microsomes and hepatocytes. The hepatocyte/microsomal CL_{int} ratio (table 4) demonstrates that only in the case of NDZ are the ratios consistently close to unity. In all situations, the 4′-HDZ ratio exceeds unity (range: 2.1–3.4), indicating that hepatocytes have greater intrinsic ability to generate this metabolite than microsomes.

***In Vivo* Studies.** Figure 3 shows plasma concentration-time profiles of DZ in typical DEX, PB, and control rats where the declines in DZ concentration are biexponential in agreement with a number of other studies (22, 23). The dose used was within the region of linear kinetics for DZ (9). A comparison of the control data ($N = 3$) with the corresponding UT data determined previously in this laboratory ($N = 6$) (9) showed that the DEX vehicle, 2% Tween 80, had no statistical effect on the terminal half-life, V_{SS}, or plasma clearance; therefore, the parameter values were combined and averaged. Volume of distribution remained unaltered in the induced states when compared with UT rats, as did half-life, whereas plasma clearance and MRT were altered significantly ($p < 0.05$) in DEX rats as a result of enzyme induction (table 5).

Intraportal administration assumes the well-stirred liver model to estimate CL_{int} (24), and using the B/P of DZ of unity (9) and the fu of DZ of 0.22 (9), the CL_{int} of this drug averages 323 and 191 ml/min/SRW in DEX and PB rats, compared with 127 ml/min/SRW in UT rats. Substantial variability is seen between individual rat values (fig. 4*A*) and, although statistical significance is reached between the UT and the DEX groups, the PB data overlap with both other groups.

Prediction of *In Vivo* CL_{int} from *In Vitro* Systems. The sum of the individual CL_{int} values for each pathway provides an estimate of

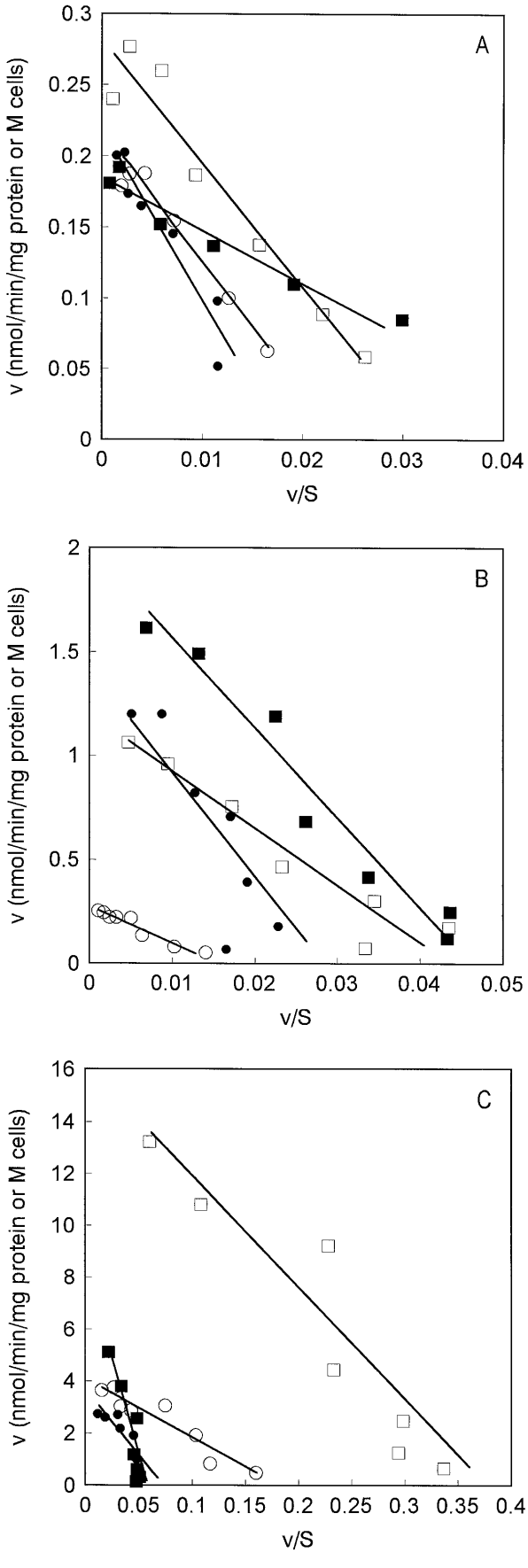

total CL_{int} *in vivo* (table 6). Neither *in vitro* system predicts the consequences of PB induction to be pronounced as the scaled CL_{int} values are <1.5-fold larger than the scaled UT values; however, DEX predictions indicate a 3-fold change in CL_{int} (fig. 4*B*). In the *in vivo* studies, changes of this magnitude are seen in the mean of the observed CL_{int} values (table 5). The hepatocyte predictions of CL_{int} in UT, PB, and DEX rats are in excellent accord with that observed *in vivo*, representing 75–92% of CL_{int}, whereas only the DEX microsomal prediction is accurate (77% of the observed value). For both the UT and PB microsomes, the predictions underestimate the *in vivo* clearance (by 64% and 57%, respectively).

Inhibition of DZ Metabolism by Its Primary Metabolites. By measuring the extent of DZ depletion in the presence of each of the exogenously added primary metabolites, the effect of product inhibition was investigated (table 7). Inhibition by 4′-HDZ is evident in both UT and induced microsomal preparations. In UT and PB microsomes, 3-HDZ and NDZ also inhibit, but to a lesser degree than 4′-HDZ. For each metabolite, the effect is more pronounced in PB than UT microsomes. In DEX microsomes, however, the effect of each metabolite differs; where 4′-HDZ inhibits, both 3-HDZ and NDZ promote DZ metabolism.

Discussion

The use of induced livers from PB- and DEX-treated rats allows the application of scaling factors to be examined in livers with differing CYP complements and zonal distribution. Thus, the general applicability of this approach to compare *in vitro* systems and to predict *in vivo* values of clearance may be challenged. In addition, the use of induced systems allows examination of conditions where particularly high clearance values would be anticipated.

Rat liver hepatocellularity has been estimated using DNA, CYP, and protein methodologies. The DNA contents measured (table 2) compare favorably with the values reported for liver of 2.2–2.5 mg/g liver (13, 17) and of 17 μg/10^6 cells reported for isolated cells (25). The resulting hepatocellularity of 85×10^6 hepatocytes/g liver in UT rats is somewhat lower than the value reported by Seglen (17) of 128×10^6 hepatocytes/g liver who also used data obtained on DNA content to calculate hepatocellularity. This discrepancy probably reflects the polyploid status of the cells, because there are known variations in cellularity and binuclearity of rats of differing ages (26). We have attempted to correct for this complication as detailed in *Materials and Methods*. The CYP content of UT isolated cells was determined as 0.31 ± 0.09 nmol/10^6 cells ($N = 4$), because rat liver contains 50 nmol of CYP/g liver (table 3); the resulting hepatocellularity (160×10^6 hepatocytes/g liver) was somewhat higher than the

FIG. 1. *Eadie-Hoftsee plots showing the relationship between the rate of metabolite formation and substrate concentration for typical PB (●) and DEX (○) hepatocyte preparations and typical PB (■) and DEX (□) microsomal preparations for 4′-HDZ (A), NDZ (B), and 3-HDZ (C).*

(*A*) For these particular microsomal preparations, V_{max} = 0.19 and 0.28 nmol/min/mg and K_M = 3.7 and 8.7 μM for PB and DEX, respectively. For these particular hepatocyte preparations, V_{max} = 0.22 and 0.22 nmol/min/M cells and K_M = 12.1 and 9.4 μM for PB and DEX, respectively. (*B*) For these particular microsomal preparations, V_{max} = 2.00 and 1.20 nmol/min/mg and K_M = 43.2 and 27.4 μM for PB and DEX, respectively. For these particular hepatocyte preparations, V_{max} = 1.42 and 0.28 nmol/min/M cells and K_M = 49.8 and 17.8 μM for PB and DEX respectively. (*C*) For these particular microsomal preparations, V_{max} = 8.51 and 16.25 nmol/min/mg and K_M = 145.2 and 43.7 μM for PB and DEX, respectively. For these particular hepatocyte preparations, V_{max} = 3.70 and 4.10 nmol/min/M cells and K_M = 50.4 and 22.4 μM for PB and DEX, respectively.

TABLE 1

Michaelis-Menten parameters for the primary pathways of DZ metabolism in hepatic microsomes and isolated hepatocytes from DEX-treated, PB-treated, and UT rats

Treatment	Pathway	Microsomes[a]			Hepatocytes[b]		
		V_{max}	K_M	CL_{int}	V_{max}	K_M	CL_{int}
		nmol/min	*μM*	*μl/min*	*nmol/min*	*μM*	*μl/min*
DEX	4′-HDZ	0.23 ± 0.07	11 ± 8	26.0 ± 10.4	0.19 ± 0.03	7 ± 3	33.4 ± 19.1
	3-HDZ	14.68 ± 1.70**	39 ± 9*	395.0 ± 136.3**	3.45 ± 0.72**	23 ± 3**†	157.5 ± 49.2**
	NDZ	1.26 ± 0.22*	23 ± 6*	58.8 ± 25.2*	0.33 ± 0.06*	14 ± 4**	24.8 ± 8.0**
PB	4′-HDZ	0.13 ± 0.04	7 ± 2	22.9 ± 17.8	0.17 ± 0.04	9 ± 3*	20.4 ± 4.3**
	3-HDZ	7.81 ± 1.18**	135 ± 27	58.5 ± 3.2**	4.67 ± 0.86**	65 ± 19†	73.2 ± 10.5**
	NDZ	2.70 ± 0.73**	54 ± 9*	50.7 ± 14.9**	1.48 ± 0.19**	56 ± 13*	26.7 ± 2.7**
UT[c]	4′-HDZ	0.16 ± 0.07	5 ± 2	39.9 ± 27.6	0.20 ± 0.05	3 ± 1	57.9 ± 9.1
	3-HDZ	2.29 ± 0.64	119 ± 32	19.1 ± 0.8	1.19 ± 0.21	71 ± 11†	17.3 ± 4.5
	NDZ	0.78 ± 0.15	35 ± 5	22.3 ± 1.9	0.25 ± 0.02	35 ± 5	7.1 ± 1.1

Data are presented as means ± SD ($N = 4$). Mean from induced states significantly different from UT (* $p < 0.05$, ** $p < 0.01$). Hepatocyte K_M significantly different from microsomal K_M († $p < 0.05$).

[a] V_{max} and CL_{int} are expressed per milligram of microsomal protein.

[b] V_{max} and CL_{int} are expressed per million cells.

[c] Data from Zomorodi *et al.* (9).

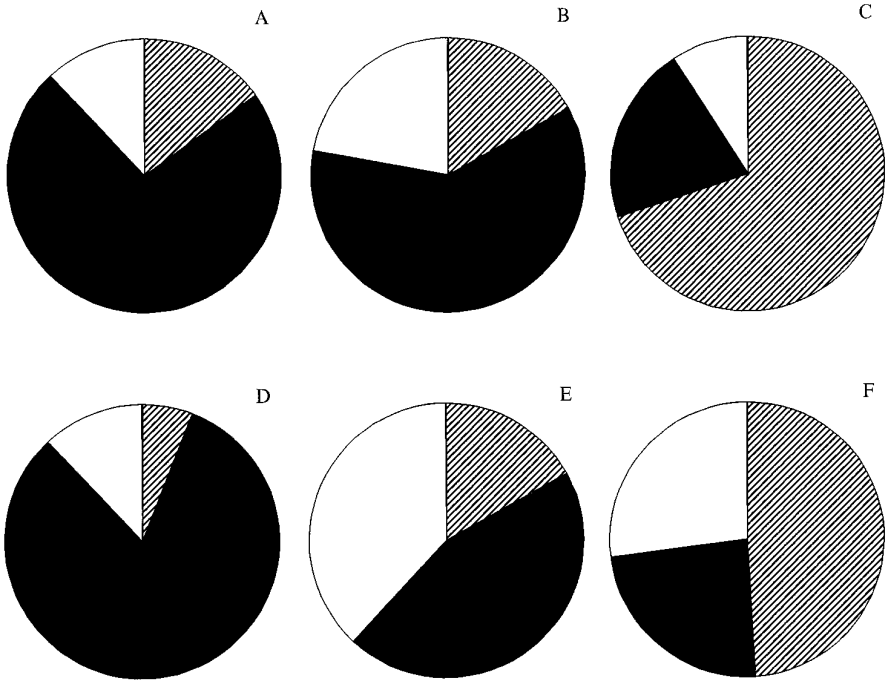

FIG. 2. *Fractions metabolized to 4′-HDZ (▨), 3-HDZ (■), and NDZ (□) in (A) DEX hepatocytes, (B) PB hepatocytes, (C) UT hepatocytes, (D) DEX microsomes, (E) PB microsomes, and (F) UT microsomes.*

Fractions calculated from the ratio of the particular CL_{int} to the sum of the three CL_{int} values.

DNA determined values. However, inaccuracies in the spectrophotometric determination of samples that are both turbid and of low CYP content compromises this approach to calculate hepatocellularity. The protein methodology yielded a UT hepatocellularity of 109×10^6 hepatocytes/g liver that is more comparable with values reported in the literature [100×10^6 cells/g (25), 95×10^6 cells/g (27), 128×10^6 cells/g (17), and 120×10^6 cells/g (28)] using a variety of methods. An advantage of the protein methodology is that no assumptions about hepatocyte characteristics like polyploidy are made and no analytical complications exist; therefore, hepatocellularities estimated by this method were adopted for future scaling of the hepatocyte data to *in vivo* units.

Microsomal protein recovery index—determined in UT, PB, and DEX microsomes—provides a scaling factor that is inversely related to the efficiency of the microsomal preparation procedure. The use of spectrophotometry to quantitate the CYP content of liver homogenate and microsomal suspensions is more applicable for these tissue samples because they contain appreciably more of the enzyme than hepatocyte suspensions for the same degree of turbidity. PB treatment caused a significant increase in the CYP content of both liver and

TABLE 2

Hepatocyte scaling factors (hepatocellularity) determined using protein and DNA methodology in UT, PB-treated, and DEX-treated rats

Treatment	DNA Content of Liver	DNA Content of Cells	Hepatocellularity[a]	Protein Content of Liver	Protein Content of Cells	Hepatocellularity[b]*
	mg/g	*μg/10^6 cells*	*10^6 hepatocytes/g liver*	*mg/g*	*mg/10^6 cells*	*10^6 hepatocytes/g liver*
UT	2.7 ± 0.3	23.7 ± 2.8	85	163.5 ± 8.0	1.5 ± 0.2	109
PB	2.6 ± 0.1	26.8 ± 5.0	73	163.4 ± 4.8	1.5 ± 0.2	109
DEX	2.7 ± 0.1	21.5 ± 4.0	94	175.6 ± 9.6	1.4 ± 0.1	125

Data are presented as means ± SD ($N = 4$ for each group). There is no statistically significant difference between either set of UT, PB, or DEX values. Protein hepatocellularity is significantly different from DNA hepatocellularity (* $p < 0.05$).

[a] Hepatocellularity calculated using DNA methodology based on ratio of liver/cell DNA content, with a correction factor of 0.75 as discussed in *Materials and Methods*.

[b] Hepatocellularity calculated using protein methodology based on ratio of liver/cell protein.

TABLE 3

Microsomal scaling factors determined in UT, PB-treated, and DEX-treated rats

	CYP Content of Liver	CYP Content of Microsomes	Microsomal Scaling Factor[a]
	nmol/g	*nmol/mg*	*mg/g liver*
UT	49.7 ± 6.8	0.8 ± 0.1	60.1
PB	71.5 ± 9.3*	1.5 ± 0.2**	46.6**
DEX	38.9 ± 7.1	0.8 ± 0.2	46.9*

Data are presented as means ± SD ($N = 4$). Mean significantly different from UT (* $p < 0.05$, ** $p < 0.01$).

[a] Microsomal scaling factor calculated from the liver/microsome ratio of CYP.

TABLE 4

Predicted CL_{int} values based on microsomal and hepatocyte incubations

Treatment	Pathway	CL_{int}		Hepatocyte/Microsomal CL_{int} Ratio
		Microsomes	Hepatocytes	
		ml/min/SRW		
DEX	4′-HDZ	13.4	45.9	3.4
	3-HDZ	203.8	216.6	1.1
	NDZ	30.3	34.1	1.1
PB	4′-HDZ	11.7	24.5	2.1
	3-HDZ	30.0	87.8	2.9
	NDZ	26.0	32.0	1.2
UT[a]	4′-HDZ	26.4	69.4	2.6
	3-HDZ	12.6	20.7	1.7
	NDZ	7.4	8.5	1.1

[a] *In vitro* data from Zomorodi *et al.* (9) scaled using the microsomal and hepatocyte scaling factors determined in tables 2 and 3.

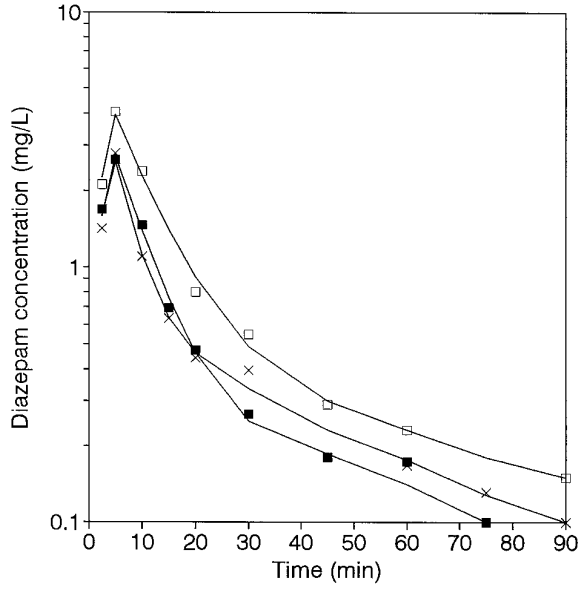

FIG. 3. *Plasma concentration-time profiles for DZ (10 mg/kg) in typical DEX (■), PB (×), and UT (□) rats after hepatic portal venous administration.*

hepatic microsomes, whereas DEX treatment had no significant effect on overall CYP levels. Because DEX caused a large increase in the rate of DZ metabolism, it is clear that some CYP isoforms were induced; therefore, the levels of other CYP isoforms must have declined. The recovery obtained for UT microsomes (60 mg/g) liver is on the upper limit of the 2-fold range previously reported (25–54 mg/g) (29–32). The scaling factors for PB and DEX of 46.6 and 46.9 mg/g liver, respectively, are lower than the corresponding UT value. Thus, we have observed similar differences within our laboratory for UT and induced livers to that seen between laboratories for the UT case. It has been reported that PB administration to rats causes an increase in hepatocyte size of almost 20% (33). This change may render the cells more susceptible to mechanical disruption, thus improving CYP recovery. These differences in microsomal recovery contrast with the invariant nature of hepatocellularity and highlight a practical issue of scaling microsomal data: the need for individualized scaling factors.

DZ was selected for the present investigation due to its CYP-mediated metabolism to the three primary products 4′-HDZ, 3-HDZ, and NDZ. We have observed marked changes in both hepatic microsomes and freshly isolated hepatocytes from PB and DEX rats, compared with UT that is consistent with the known involvement of several CYP isoforms. The role of the CYP3A subfamily in 3-HDZ formation is evident in the large increase in CL_{int} for this pathway after DEX treatment in both *in vitro* systems. Interestingly, DEX treatment resulted in a 50% reduction of the 3-HDZ pathway K_M in both microsomes and hepatocytes, whereas this parameter remained unaltered after PB treatment. In our study, both inducer treatments resulted in an increase in the NDZ CL_{int} in both *in vitro* systems, indicating an important role for the CYP2B and CYP3A subfamilies in this pathway. The lack of any induction of the 4′-aromatic hydroxylation of DZ in the present study supports the claim that this pathway is catalyzed by CYP2D1. In the microsomal preparations there is no substantial difference between either of the kinetic param-

TABLE 5

Pharmacokinetic parameters for DZ disposition in UT, PB-treated, and DEX-treated rats

	V_{SS}	MRT	Terminal $t_{1/2}$	Plasma *CL*	CL_{int}
	liters/SRW	*min*	*min*	*ml/min/SRW*	*ml/min/SRW*
UT	1.1 ± 0.5	51.3 ± 31.4	38 ± 18	31 ± 10	127 ± 58
PB	1.2 ± 0.5	42.3 ± 18.7	39 ± 15	41 ± 32	191 ± 154
DEX	0.8 ± 0.3	10.2 ± 2.7*	21 ± 7	71 ± 26*	323 ± 108**

Data are presented as means ± SD ($N = 9$ for UT and $N = 5$ for PB and DEX). Mean significantly different from UT and PB (* $p < 0.05$). Mean significantly different from UT (** $p < 0.05$).

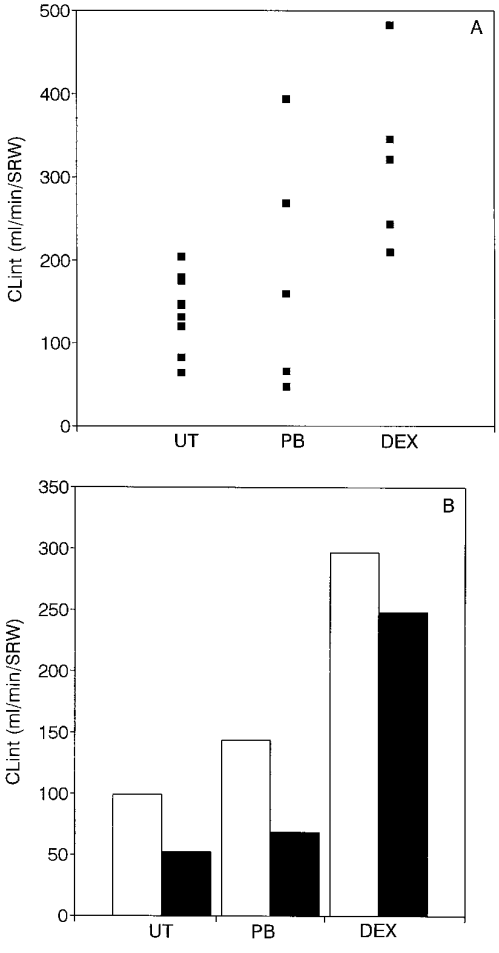

FIG. 4. *Observed (A) and predicted (B) CL_{int} of DZ in UT, PB, and DEX rats.*

Data for individual rats are shown in (*A*). Predictions from microsomal (■) and hepatocyte (□) studies are shown in (*B*).

eters for PB and DEX, compared with UT (table 1). A similar effect in hepatocytes for DEX is observed, but for PB, there is a statistically significant decrease in CL_{int} due to an increase in K_M. We have no explanation for this observation, but it should be remembered that K_M is an apparent value representing the ratio of several rate constants.

Although the consequences of induction on DZ clearance *in vivo* are quantitatively well predicted from both hepatocytes and microsomes (92% and 77% accuracy, respectively) in the DEX case, only hepatocytes accurately (75%) predict the PB case. This clearly demonstrates the value of the hepatocyte scaling factor determined after the induction treatments and confirms that freshly isolated hepatocytes consistently provide reliable estimates of *in vivo* CL_{int}. To date, we have demonstrated successful hepatocyte predictions over a range

TABLE 6

In vivo and scaled microsomal- and hepatocyte-predicted DZ CL_{int} values

Treatment	CL_{int}		
	In Vivo	Microsomal[a]	Hepatocyte[a]
		ml/min/SRW	
UT	127	54 (43%)	99 (78%)
PB	191	68 (36%)	144 (75%)
DEX	323	248 (77%)	297 (92%)

Numbers in parentheses represent percentage of *in vivo* CL_{int}.

[a] Obtained by scaling *in vitro* CL_{int} by 513, 513, and 660 mg/SRW for PB, DEX, and UT microsomes, respectively, and 1.2, 1.4, and 1.2 × 10^9/SRW for PB, DEX, and UT hepatocytes, respectively. UT predictions differ from previous publication (7) due to the use of literature scaling factors in the previous study.

TABLE 7

Modulation of microsomal DZ metabolism by 4′-HDZ, 3-HDZ, and NDZ

Treatment	% Change[a]		
	4′-HDZ	3-HDZ	NDZ
UT	−34 ± 3	−25 ± 6	−27 ± 2
PB	−64 ± 5	−46 ± 6	−50 ± 4
DEX	−66 ± 4	+31 ± 20	+141 ± 78

Data are presented as means ± SD ($N = 4$ for each treatment).

[a] Refers to change in control rate of DZ depletion (2 μM) in the presence of metabolite (100 μM). Control rates were 0.097 ± 0.004, 0.137 ± 0.008, and 0.155 ± 0.007 nmol/min/mg for UT, PB, and DEX microsomes, respectively.

of 2 orders of magnitude, from 2.4 ml/min/SRW for tolbutamide (35) to the value obtained in the present DEX study of 297 ml/min/SRW and including 16 other drugs (1).

The underprediction from PB microsomes is similar to that previously observed for UT microsomes (fig. 4), and we have speculated that this is a consequence of endproduct inhibition (9)—a phenomenon demonstrated for DZ in isolated perfused liver preparations (34). In the present study, we have examined this proposal further and have demonstrated that whereas all three primary metabolites are capable of inhibiting DZ metabolism, 4′-HDZ is the more effective. In UT hepatocytes the 4′-HDZ pathway dominates, representing 70% of CL_{int}, whereas in microsomes the corresponding contribution is only 49%. This effect can be seen in the hepatocyte/microsomal CL_{int} ratio of 2.6 in table 4. PB microsomes also underpredict *in vivo* clearance and a similar inhibitory effect may occur. Although the rates of formation of the three metabolites are more equally balanced in PB than in UT microsomes, the metabolite inhibitory effects are greater in the former case. In DEX microsomes, 4′-HDZ is also inhibitory, and the hepatocyte/microsomal CL_{int} ratio is 3.4 for the 4′-HDZ pathway. However, this pathway is of minor importance after DEX induction (fig. 2) and hence the phenomenon is of little importance. Interestingly, 3-HDZ and, in particular, NDZ stimulate DZ metabolism. The

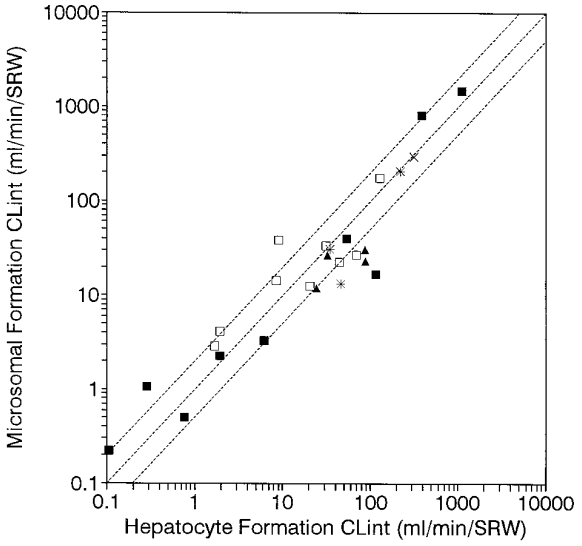

FIG. 5. *Relationship between microsomal CL_{int} and hepatocyte CL_{int} for 12 drugs by 26 pathways.*

Data are from table 1 and refs. 1, 9, 10, 35, and 38. *Dotted lines* represent the lines of identity, a 50% underprediction, and a 100% overprediction. Data shown are from our laboratory for UT (□), PB (▲), DEX (∗) (scaling factors from tables 2 and 3), and β-naphthoflavone (×) (scaling factors from ref. 38), and from other laboratories for UT (■) (scaling factors from ref. 1).

latter metabolite is known to undergo CYP3A-catalyzed oxidation (6) and there are several examples of substrate activation for this particular CYP isoform (36, 37). However, 3-HDZ, the major metabolite accounting for some 80% of CL_{int} in DEX rats, has only a minor effect in these microsomes. Thus, the modulating effects of these metabolites on predicting the overall DZ clearance would be manifest only for the UT and PB microsomes. The presence of fully functional phase 2 enzymes in the intact hepatocyte would minimize the accumulation of the CYP-formed primary metabolites; thus product inhibition would not be anticipated in this *in vitro* system (9).

The successful prediction from DEX microsomes for DZ is of particular interest. The most accurate microsomal predictions of CL_{int} have previously been confined to compounds with a low CL_{int} such as caffeine (2.7 ml/min/SRW) (10) and tolbutamide (3.1 ml/min/SRW) (35). The predictions for many drugs with a high CL_{int} has been poor (1), and this has led to speculation that an upper limit may exist for microsomal turnover. However the results of the present study unequivocally demonstrate that this widely used *in vitro* system can accurately estimate high *in vivo* CL_{int} values, because the DEX prediction was 77% of the actual value. The suggestion of a nonlinear relationship between microsomal *CL* and hepatocyte *CL* is refuted by the present analysis and thus the reason for previous underpredictions may be isoform/pathway-dependent, rather than a result of the existence of an upper limit of metabolism rates in microsomes.

The results presented herein enable a detailed comparison of the utility of both microsomal and hepatocyte predictions of CL_{int}. These data, together with data previously reported (1, 9, 10, 35, 38), total some 12 CYP substrates with ethoxycoumarin and DZ being studied in various CYP induction states. A number of these compounds are metabolized *via* two or more primary routes, and thus there is corresponding microsomal and hepatocyte data concerning some 26 pathways. Figure 5 presents the CL_{int} data, scaled to *in vivo* units using the appropriate scaling factors (tables 2 and 3), with *dotted lines* representing the line of identity, a 50% underprediction of CL_{int}, and a 100% overprediction of CL_{int}. The data range over 4 orders of magnitude, and the level of similarity in CL_{int} predictions between the two *in vitro* systems is impressive, given the varied sources of data and the use of CYP inducers that have marked effects on the liver. There are only five pathways that exhibit a marked underprediction in microsomes, compared with hepatocytes, and three of these refer to DZ 4′-hydroxylation in UT, PB, and DEX states, probably due to endproduct inhibition. Therefore, inherently, both microsomes and hepatocytes can be regarded as equally valuable tools to predict *in vivo* pharmacokinetic behavior, because the majority of compounds exhibit similar scaled CL_{int} values in both systems.

The present study exemplifies how both hepatic microsomes and freshly isolated hepatocytes can be used to predict *in vivo* CL_{int} when easily determined scaling factors are used. The UT microsomal scaling factor determined in this study (660 mg/SRW) is higher than the value of 500 mg/SRW proposed earlier (1), based on literature reports. However, this value is on the upper limit of the 2-fold range of microsomal recovery reported of 275–600 mg/SRW (1). This range in reported values is not surprising, because this parameter is a direct measure of the efficiency of the microsomal preparation procedure that will vary between laboratories according to the details of the methods used. In addition, the estimated hepatocellularity (1.2×10^9/SRW) is slightly lower than the corresponding value of 1.5×10^9/SRW proposed earlier (1), although once again it is within the range of reported hepatocellularities ($1.1–1.5 \times 10^9$ cells/SRW). The comparatively small range (30%) for this latter scaling factor indicates that, for successful scaling of hepatocyte data, it is not necessary for individual laboratories to determine their own scaling factor, because hepatocellularity is not an experimental variable. In contrast, microsomal protein recovery seems to be laboratory-dependent; therefore, individual laboratories should determine their own scaling factor to maximize the predictive utility of their microsomal data.

Acknowledgments. We gratefully acknowledge the skilled assistance of Beverley Brennan in a portion of this work.

References

1. J. B. Houston: Utility of *in vitro* drug metabolism data in predicting *in vivo* metabolic clearance. *Biochem. Pharmacol.* **47,** 1469–1479 (1994).
2. F. P. Guengerich, G. A. Dannan, S. T. Wright, M. V. Martin, and L. S. Kaminsky: Purification and characterization of liver microsomal cytochromes-P450: electrophoretic, spectral, catalytic, and immunochemical properties and inducibility of eight isozymes isolated from rats treated with phenobarbital or β-naphthoflavone. *Biochemistry* **21,** 6019–6030 (1982).
3. D. L. Simmons, P. McQuiddy, and C. B. Kasper: Induction of the hepatic mixed-function oxidase system by synthetic glucocorticoids. Transcriptional and posttranslational regulation. *J. Biol. Chem.* **262,** 326–332 (1987).
4. D. M. Heuman, E. J. Gallagher, J. L. Barwick, N. A. Elshourbagy, and P. S. Guzelian: Immunochemical evidence for induction of a common form of hepatic cytochrome P-450 in rats treated with pregnenolone-16α-carbonitrile or other steroidal or nonsteroidal agents. *Mol. Pharmacol.* **21,** 753–760 (1982).
5. R. Gebhardt: Metabolic zonation of the liver: regulation and implications for liver function. *Pharmacol. Ther.* **53,** 275–354 (1992).
6. P. E. B. Reilly, D. A. Thompson, S. R. Mason, and W. D. Hooper: Cytochrome P450IIIA enzymes in rat liver microsomes: involvement in C_3-hydroxylation of diazepam and nordazepam but not N-dealkylation of diazepam and temazepam. *Mol. Pharmacol.* **37,** 767–774 (1990).
7. C. F. Neville, S. Ninomiya, N. Shimada, T. Komataki, S. Imaoka, and Y. Funae: Characterization of specific cytochrome P450 enzymes responsible for the metabolism of diazepam in hepatic microsomes of adult male rats. *Biochem. Pharmacol.* **45,** 59–65 (1993).

8. H. O. Jauregui, S. F. Ng, K. L. Gann, and D. J. Waxman: Xenobiotic induction of P450 PB-4 (IIB1) and P450c (1A1) and associated monooxygenase activities in primary cultures of adult rat hepatocytes. *Xenobiotica* **21,** 1091–1106 (1991).
9. K. Zomorodi, D. J. Carlile, and J. B. Houston: Kinetics of diazepam metabolism in rat hepatic microsomes and hepatocytes and their use in predicting *in vivo* clearance. *Xenobiotica* **25,** 907–916 (1995).
10. K. A. Hayes, B. S. Brennan, R. Chenery, and J. B. Houston: *In vivo* disposition of caffeine predicted from hepatic microsomal and hepatocyte data. *Drug Metab. Dispos.* **23,** 349–353 (1995).
11. T. Omura and R. Sato: The carbon monoxide binding pigment of liver microsomes. *J. Biol. Chem.* **239,** 2370–2378 (1964).
12. O. H. Lowry, N. J. Rosebrough, A. L. Farr, and R. J. Randall: Protein measurement with the Folin phenol reagent. *J. Biol. Chem.* **193,** 265–275 (1951).
13. T. R. Downs and W. W. Wilfinger: Fluorometric quantification of DNA in cells and tissue. *Anal. Biochem.* **131,** 538–547 (1983).
14. J. C. Y. Dunn, M. L. Yormush, H. G. Koebe, and R. G. Tompkins: Hepatocyte function and extracellular matrix geometry: long term culture in a sandwich configuration. *FASEB J.* **3,** 174–177 (1989).
15. H. Akrawi and P. J. Wedlund: Method for chronic portal vein infusion in unrestrained rats. *J. Pharmacol. Methods* **17,** 67–74 (1987).
16. P. G. Harns and S. R. Ojeda: A rapid and simple procedure for chronic cannulation of the rat jugular vein. *J. Appl. Physiol.* **36,** 391–392 (1974).
17. P. O. Seglen: Preparation of rat liver cells. *Exp. Cell. Res.* **82,** 391–398 (1973).
18. P. Steinberg, W. M. Lafranconi, C. R. Wolf, D. J. Waxman, F. Oesch, and T. Friedberg: Xenobiotic metabolizing enzymes are not restricted to parenchymal cells in rat liver. *Mol. Pharmacol.* **32,** 463–470 (1987).
19. F. P. Guengerich: Similarity of nuclear and microsomal cytochromes P450 in the *in vitro* activation of aflatoxin B1. *Biochem. Pharmacol.* **28,** 2883–2890 (1979).
20. H. Mukhtar, T. H. Elmalouk, R. M. Philpot, and J. R. Bend: Rat hepatic nuclear cytochrome P-450 and epoxide hydrase in membranes prepared by 2 methods. Similarities with the microsomal enzymes. *Mol. Pharmacol.* **15,** 192–196 (1979).
21. W. Stäubli, R. Hess, and E. R. Weibel: Correlated morphometric and biochemical studies on the liver cell. II. Effects of phenobarbital on rat hepatocytes. *J. Cell Biol.* **42,** 92–112 (1969).
22. U. Klotz, K. H. Antonin, and P. R. Bieck: Pharmacokinetics and plasma binding of diazepam in man, dog, rabbit, guinea pig and rat. *J. Pharmacol. Exp. Ther.* **199,** 67–73 (1976).
23. C. F. C. Tsang and G. R. Wilkinson: Diazepam disposition in mature and aged rabbits and rats. *Drug Metab. Dispos.* **10,** 413–416 (1982).
24. G. R. Wilkinson: Clearance approaches in pharmacology. *Pharmacol. Rev.* **39,** 1–47 (1987).
25. M. N. Berry, A. M. Edwards, and G. J. Barritt: "Isolated Hepatocytes, Preparation, Properties and Applications," p. 27. Elsevier, Oxford, 1991.
26. D. N. Wheatley: Binucleation in mammalian liver. Studies on the control of cytokines *in vivo*. *Exp. Cell Res.* **74,** 455–465 (1972).
27. O. Greengard, M. Federman, and W. E. Knox: Cytomorphometry of developing rat liver and its application to enzymic differences. *J. Cell Biol.* **52,** 261–272 (1972).
28. R. N. Zahlten and F. W. Stratman: The isolation of hormone-sensitive rat hepatocytes by a modified enzymatic technique. *Arch. Biochem. Biophys.* **163,** 600–608 (1974).
29. W. Grosse and A. E. Wade: The effect of thiamine consumption on liver drug-metabolizing pathways. *J. Pharmacol. Exp. Ther.* **205,** 596–605 (1978).
30. D. L. Cinti and J. B. Schenkman: Hepatic organelle interaction. I. Spectral investigation during drug biotransformation. *Mol. Pharmacol.* **8,** 327–338 (1972).
31. J.-G. Joly, C. Doyon, and Y. Pesant: Cytochrome P-450 measurement in rat liver homogenate and microsomes. Its use for correction of microsomal losses incurred by differential centrifugation. *Drug Metab. Dispos.* **3,** 577–586 (1975).
32. C. Bäärnhielm, H. Dahlbäck, and I. Skånberg: *In vivo* pharmacokinetics of felodipine predicted from *in vitro* studies in rat, dog and man. *Acta Pharmacol. Toxicol.* **59,** 113–122 (1986).
33. K. Tonda, T. Hasegawa, and M. Hirata: Effects of phenobarbital and 3-methylcholanthrene pretreatments on monooxygenase activities and proportions of isolated rat hepatocyte subpopulations. *Mol. Pharmacol.* **23,** 235–243 (1983).
34. E. M. Savenije-Chapel, A. Bast, and J. Noordhoek: Inhibition of diazepam metabolism in microsomal- and perfused liver preparations of the rat by desmethyldiazepam, N-methyloxazepam and oxazepam. *Eur. J. Drug Metab. Pharmacokinet.* **10,** 15–20 (1985).
35. E. I. L. Ashforth, D. J. Carlile, R. Chenery, and J. B. Houston: Prediction of *in vivo* disposition from *in vitro* systems: clearance of phenytoin and tolbutamide using rat hepatic microsomal and hepatocyte data. *J. Pharmacol. Exp. Ther.* **274,** 761–766 (1995).
36. Y.-F. Ueing, T. Kuwabara, Y.-J. Chun and F. P. Guengerich: Cooperativity in oxidations catalyzed by cytochrome P450 3A4. *Biochemistry* **36,** 370–381 (1997).
37. M. Shou, J. Grogan, J. A. Mancewicz, K. W. Krausz, F. J. Gonzalez, H. V. Gelboin, and K. R. Korzekwa: Activation of CYP3A4: evidence for the simultaneous binding of two substrates in a cytochrome P450 active site. *Biochemistry* **33,** 6450–6455 (1994).
38. D. J. Carlile, M. Dickins, and J. B. Houston: Scaling factors for predicting the kinetics of drug metabolism *in vivo* using *in vitro* systems. *Br. J. Clin. Pharmacol.* **38,** 177P (1994).